

Windowless high power liquid-metal targets: theoretical assessments and numerical modelling

S. Gordeev, V. Heinzl, R. Stieglitz, L. Stoppel

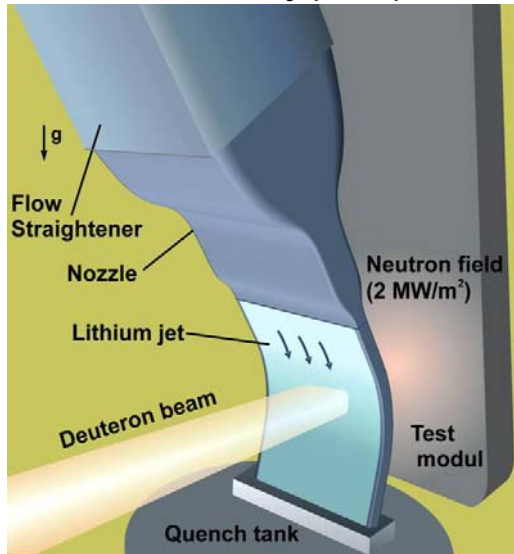


4th High Power Targetry Workshop
Malmö - Sweden, May 2nd – 6th, 2011

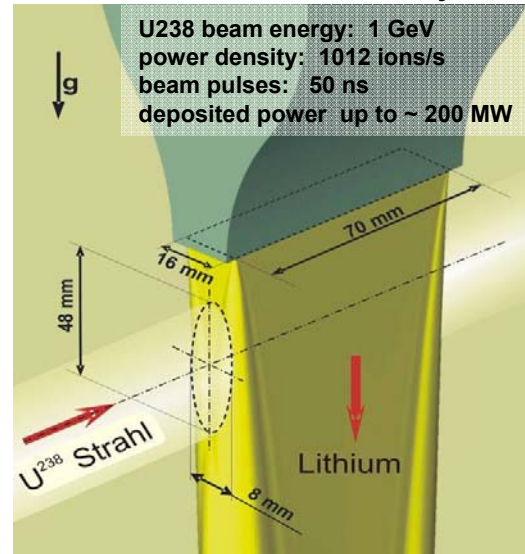
- **Windowless high power liquid-metal targets**
- **Factors influencing the stability of the free surface flow in liquid metal targets**
- **Analytical assessment of the free surface flow instabilities**
- **Numerical simulations and validation of CFD models**
- **Conclusions**

Windowless high power liquid-metal targets

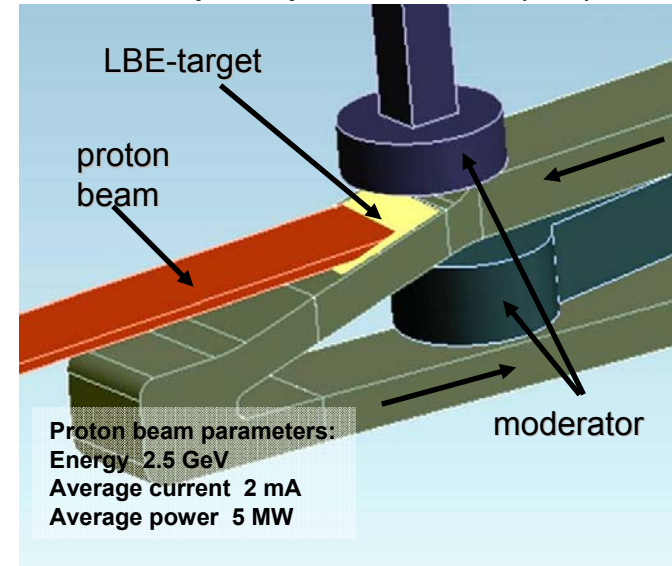
International Fusion Materials Irradiation Facility (IFMIF)



Fragment Separator Super-FRS of the FAIR accelerator facility



Free-surface target for European Spallation Source (ESS)



- The problem of high-power heat removal exists for many accelerator projects (IFMIF, Super-FRS, Franz...) .
- A technical option to overcome the material temperature limitation is given by considering free-surface liquid-metal targets.
- Liquid-metal target is acting as a target to generate the secondary particles but also to remove the heat originating from the production process.

Requirements to the (LM) target design:

- Removal of the deposited beam energy
- Avoiding of over-heating and irradiation of the target structure
- Avoiding of corrosion / erosion of the target structure



Requirements to the hydro-dynamic stability of the liquid metal jet

Instability mechanisms (sources) in the target flow

I. Influence of the nozzle geometry

a) Nozzle edge (corner, obstacles, etc)

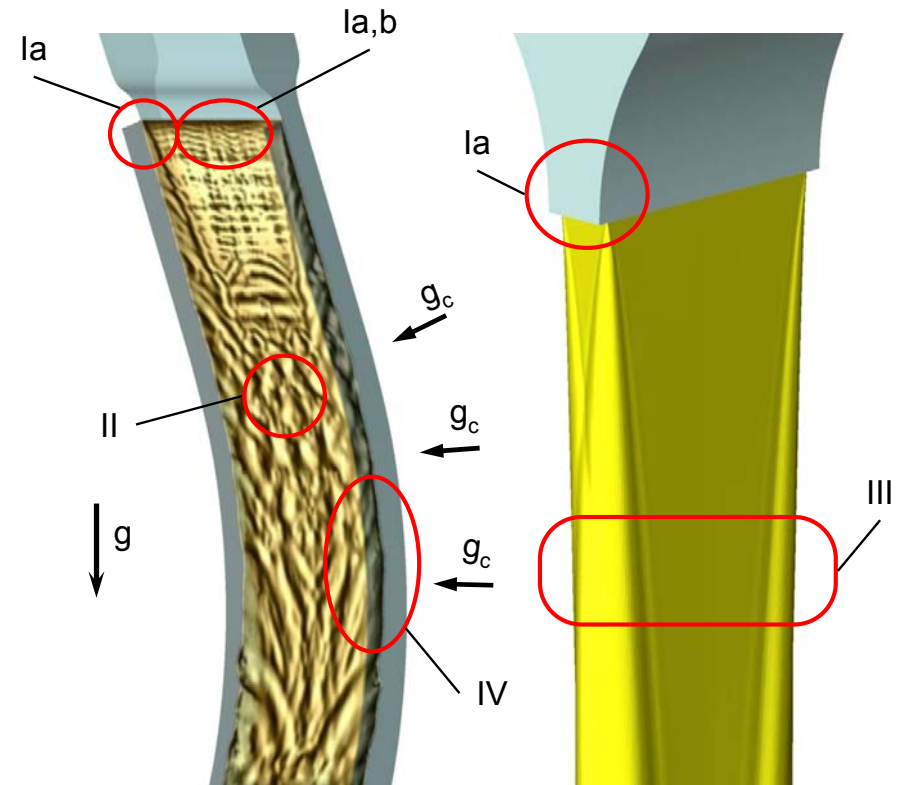
c) Boundary layer relaxation at the nozzle outlet.

II. Turbulence transport to the free surface

III. Surface tension

IV. Effect of centrifugal acceleration

Gravitation waves, hydraulic jump, secondary flows.



- Analytical methods treat these effects separately.
Only CFD simulation can reproduce the complete condition of the free surface flow .
- Detailed validation of CFD models against analytical estimations and experimental data is necessary.

Validation of turbulence models. Numerical methods

- **CFD codes: Star-CD, Star-CCM+**
- **Turbulence models:**
 - **RANS (Reynolds Averaged Navier-Stokes) model: V2F four-equation turbulence model;**
 - **LES (Large Eddy Simulation) model: Wall-adapting local eddy-viscosity Subgrid-Scale model (WSG);**
- **Free Surface modelling:**
 - **Volume of Fluid method (VOF)**
 - **Sharp gas-liquid interface computed using High- Resolution Interface-Capturing (HRIC) scheme.**
 - **Transient analysis option are used for computing of free surface flow**

Free surface instabilities.

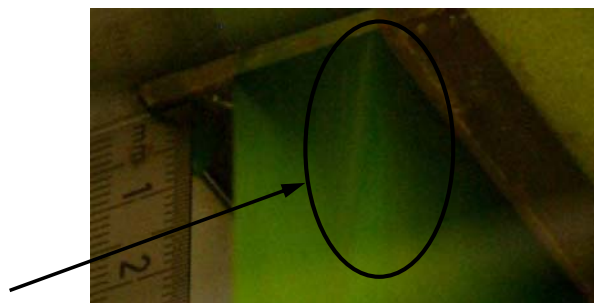
I. Standing waves:

- Waves caused by steady disturbances (obstacles, corners, stable vortices)

II. Traveling pattern on the free surface:

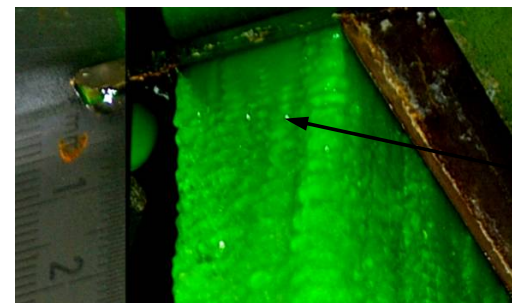
- Waves induced by the change of the velocity profile in the boundary layer flow during the transition from the wall shear flow to the shear stress free flow.
- Interaction of turbulent structures with free surface

Free surface structure of the water jet flow near the nozzle exit ($U_0=5\text{m/s}$), (KIT, Stoppel, 2008)



Standing waves

Exposure time ca. 4 ms



Traveling waves

Exposure time ca. 50 μs

Standing waves. Analytical estimation

Analytical estimation of the wave pattern shape

Phenomenology:

- Geometry discontinuity at nozzle exit
- Convective instability downstream

Description of the wave pattern shape evolution :

correlations for the iso-phase lines of the wave pattern :

$$y = p \cos \theta - \frac{dp}{d\theta} \sin \theta, \quad x, z = p \sin \theta + \frac{dp}{d\theta} \cos \theta$$

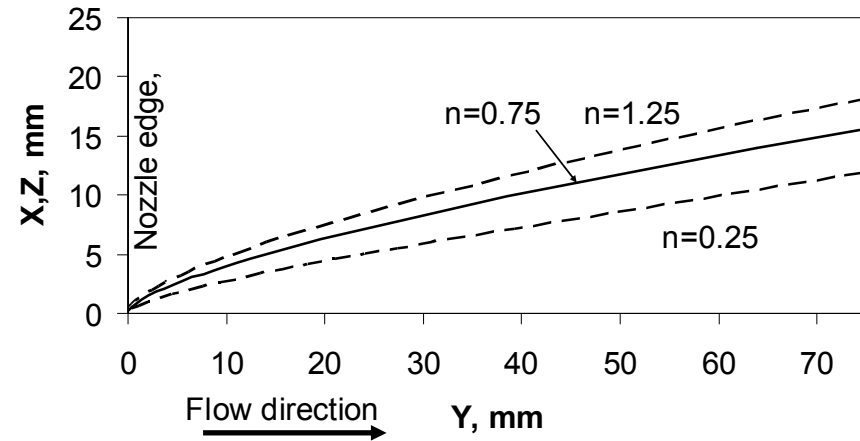
- p is the distance between a point on the wake and a source of disturbance
- θ is the angle between the ray p and the axis Y

where n is an integer denotes the phase of the wake ($n=0.25; 1.25$ – crests, $n=0.75; 1.75$ – troughs) , λ is the wavelength.

$$p = n \cdot \lambda$$

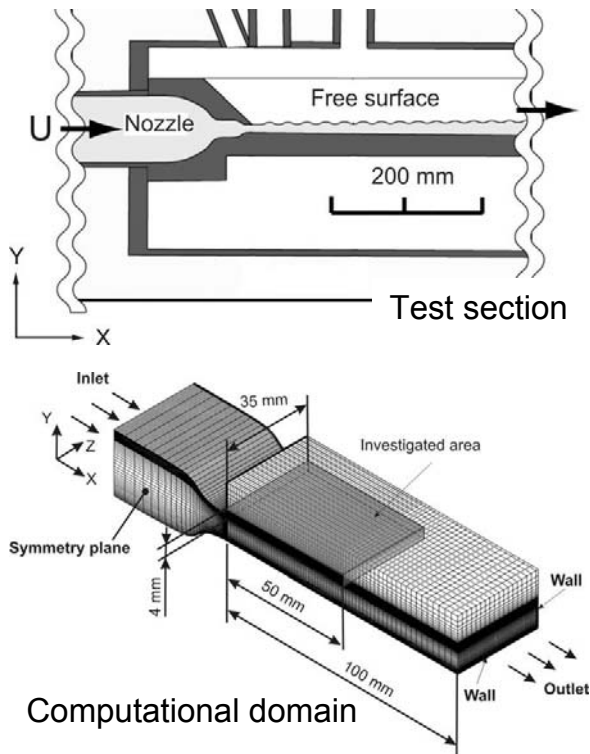
where c is the phase velocity, U is flow velocity , ρ is the density, σ is surface tension and d is the depth of the fluid.

$$\theta = \sin^{-1} \left(\frac{c}{U} \right), \quad c = \sqrt{\left(\frac{g\lambda}{2\pi} + \frac{2\pi\sigma}{\lambda\rho} \right) \tanh \frac{2\pi D}{\lambda}}$$

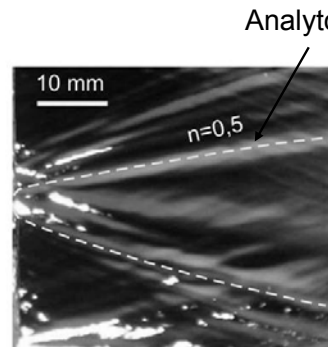


Standing waves. Waves caused by obstacles

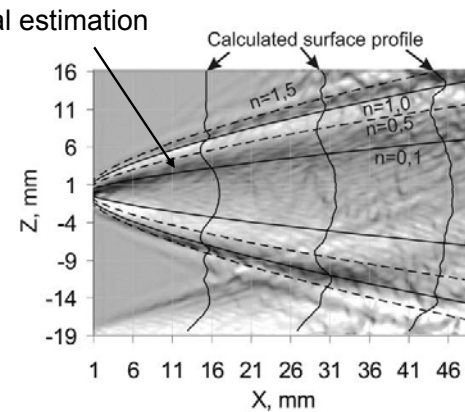
Capillary waves generated by particles of chemical compounds attached at the nozzle edge,
 Lithium Experiments, Osaka Un.
 Kondo et al. (2006)



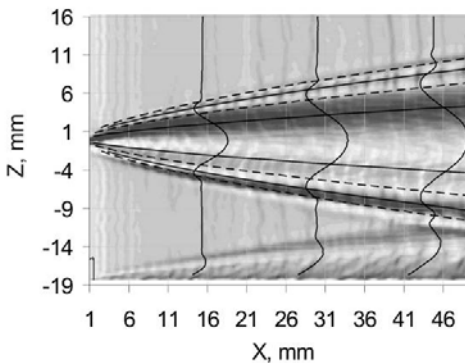
Experiment



LES*

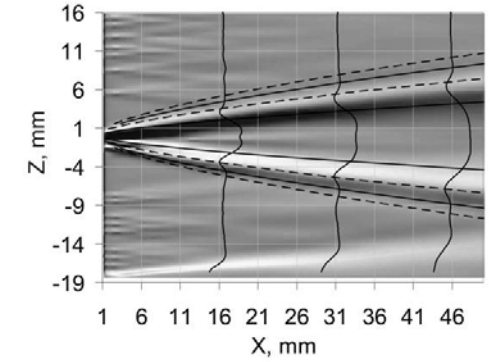
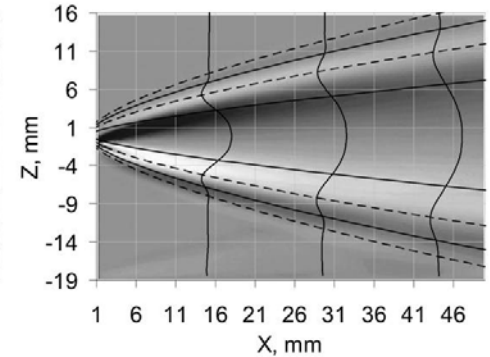


Flow velocity $U=5\text{m/s}$



Flow velocity $U=10\text{m/s}$

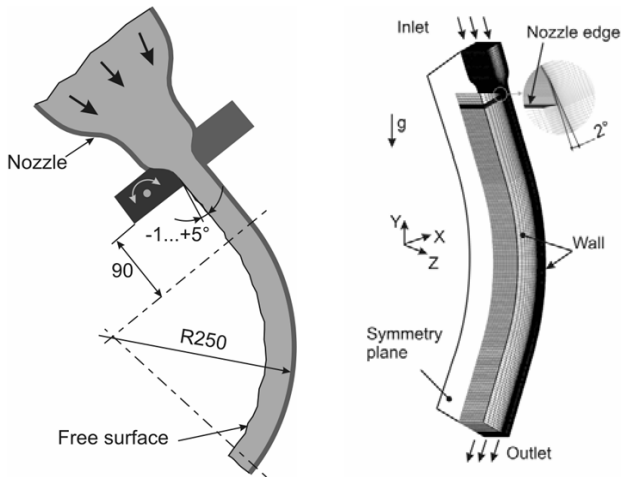
RANS* (V2F)



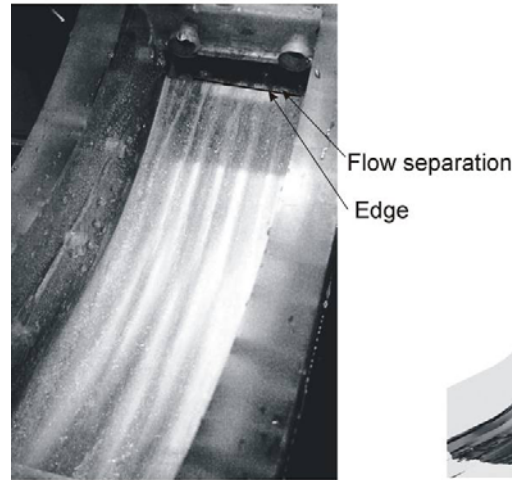
* Reynolds Averaged Navier-Stokes (RANS), Large Eddy Simulation (LES)

Standing waves. Waves caused by Taylor-Görtler vortices

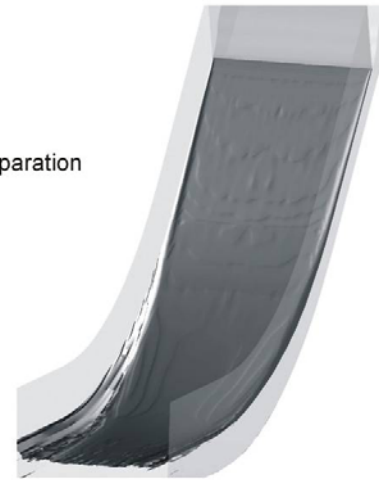
Waves generated by flow separation at the divergent nozzle wall. Water experiments, IPPE, Loginov et al. (2006), flow velocity $U=10\text{m/s}$



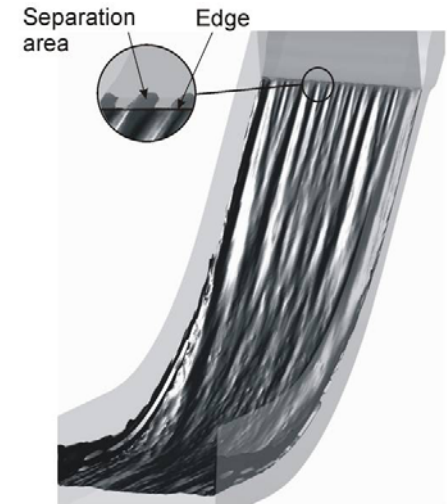
Experiment



RANS (V2F)

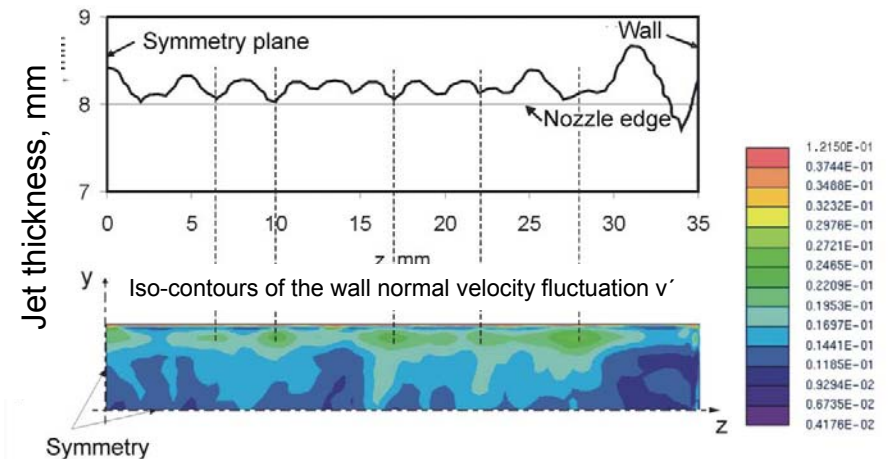


LES



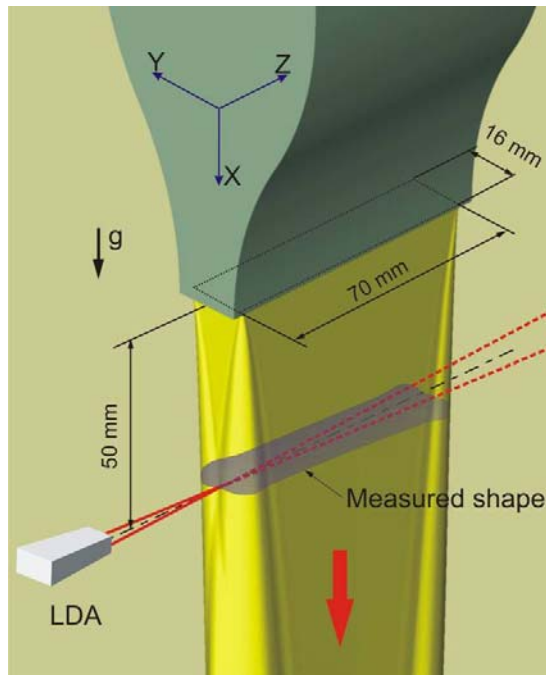
Free surface of the water jet 5 mm downstream from the nozzle exit

- Important result of LES simulations - local flow separation on the divergent wall is influenced from wall normal velocity fluctuations.
- In all probability the reason is Goertler-Taylor Instability in the concave part of the nozzle (Goertler number $Go \approx 12 > Go_{cr}=7$)
- This kind of waves can appear on the eroded nozzle edge of the target

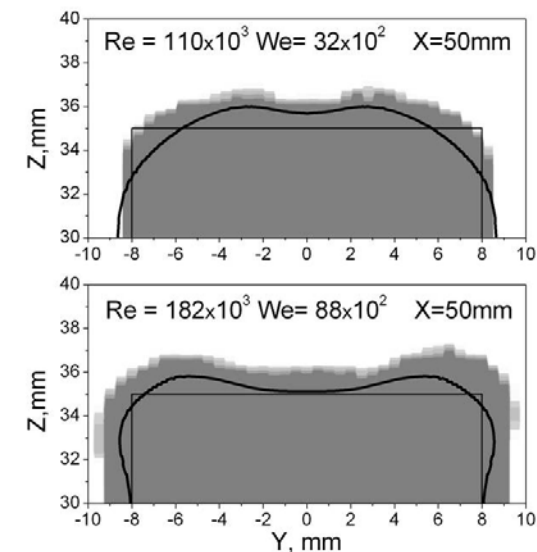
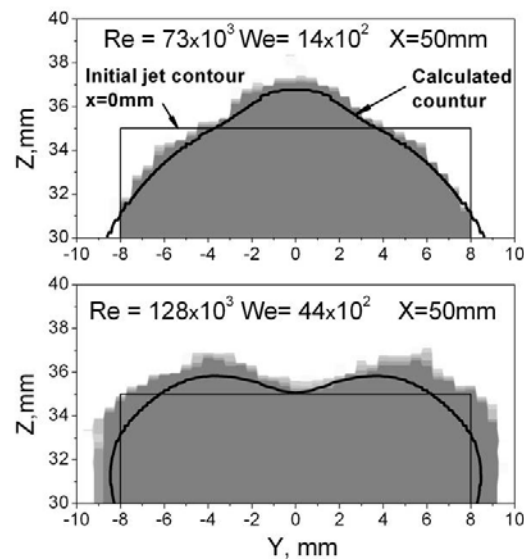


Standing waves. Alteration of the jet cross section caused by standing waves and surface tension.

LDA measurements of the jet cross section contour (KIT, KALLA, Stoppel, 2007)



The data recorded in form of 2D-matrix of concentration of the LDA-particles compared with CFD simulations (RANS, V2F)

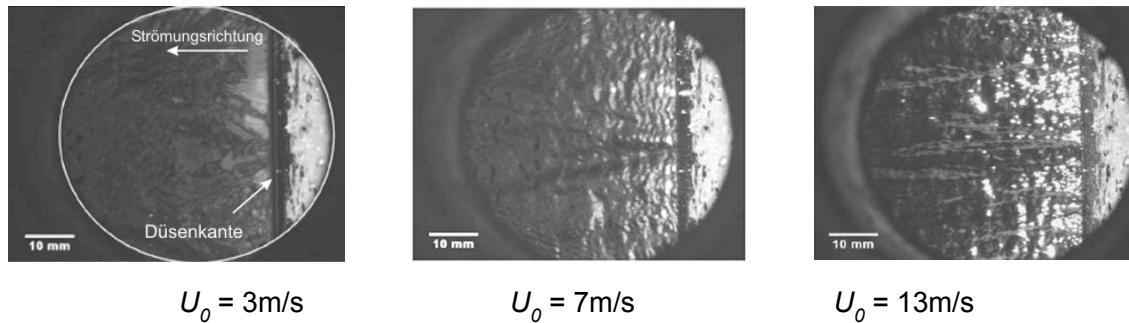


The deviation between the experimental data and simulation results is less than 8%

Traveling patterns. Waves caused by boundary layer relaxation. Analytical estimation

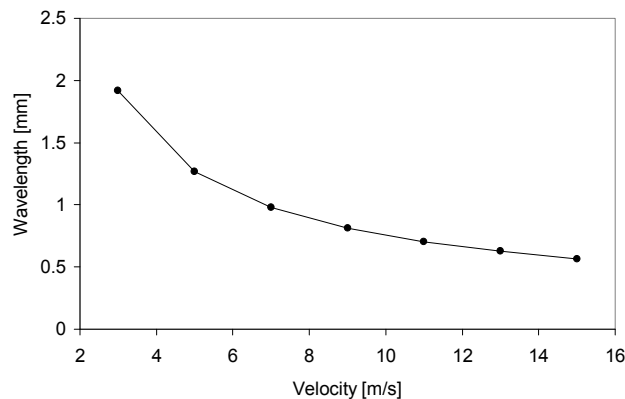
Traveling pattern on the free surface induced by the change of the velocity profile in the boundary layer flow during the transition from the wall shear flow to the shear stress free flow.

Free surface structure of the lithium flow near the nozzle exit, Osaka Un., Kondo et al. (2005)



For lithium flow in Osaka Un. test section Reynolds Number based on momentum thickness $Re_{\delta_2} = 160 - 600 > Re_{\delta_2}^{cr} \approx 70$ (Brennen, 1968). Onset of this kind of waves is expected.

Wave length as function of mean velocity at the nozzle exit for Osaka Un. test section

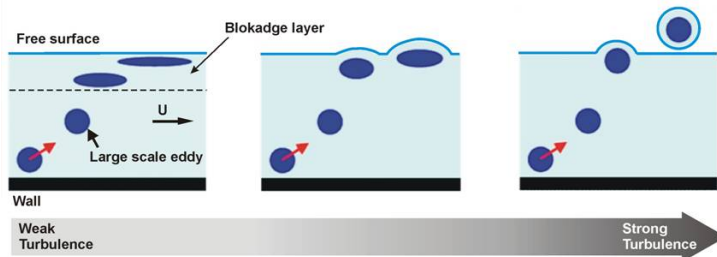


Relation between dimensionless wave number α and Reynolds number based on momentum thickness Re_{δ_2} , Hagsberger (1983):

$$\alpha = \exp\left(-9,6481 + 2,4412 \ln(Re_{\delta_2}) - 0,1762 \ln^2(Re_{\delta_2})\right)$$

$$\alpha \equiv 2\pi \delta_2 / \lambda$$

Traveling patterns. Turbulence transport to the free surface. Analytical estimation



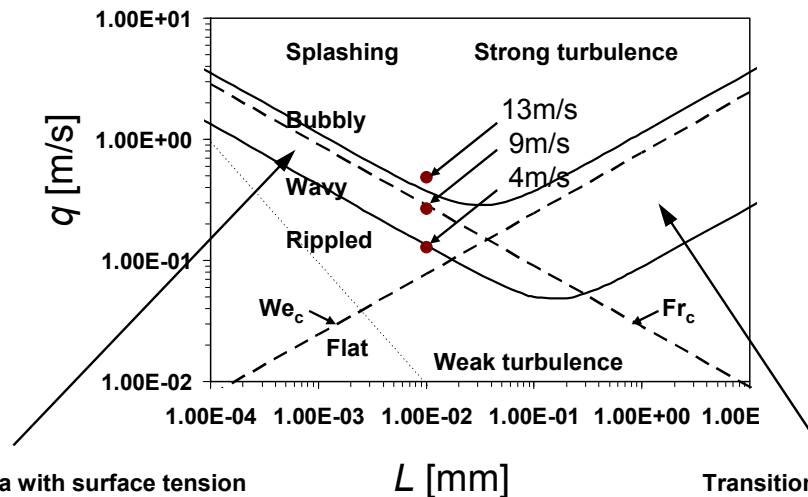
L-q Diagram adapted from Brocchini und Peregrine (2001)

q – velocity scale, velocity of a typical turbulent element near the free surface. ($U_\tau = (\tau_w / \rho)^{0.5}$),

L - length scale (film thickness) of a typical turbulent element

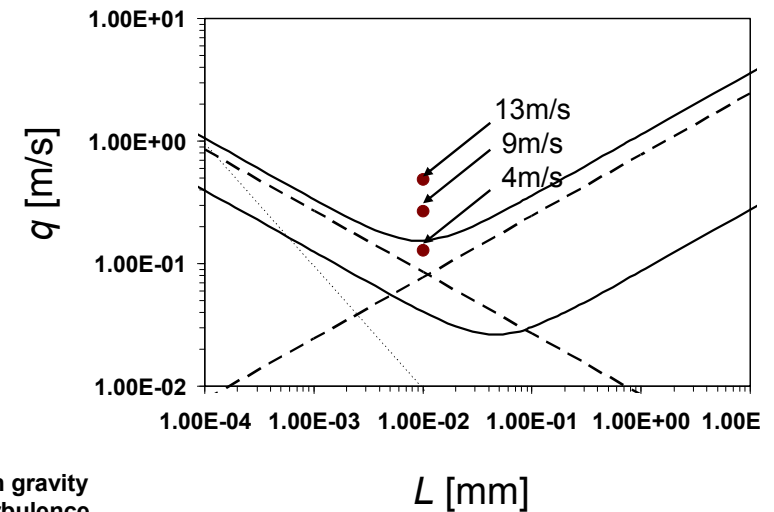
Osaka Un. Li Experiments (2005-2010)
 2d waves observed for $U > 5\text{m/s}$
 3d irregular waves observed for $U > 11\text{m/s}$

Nagoya Un. Water Experiments (Itoh et al., 1999)
 Waves observed for $U > 3\text{m/s}$
 3d irregular waves observed for $U > 11\text{m/s}$



Transition area with surface tension dominance over turbulence

Transition area with gravity dominance over turbulence



Traveling patterns. Validation of turbulence models

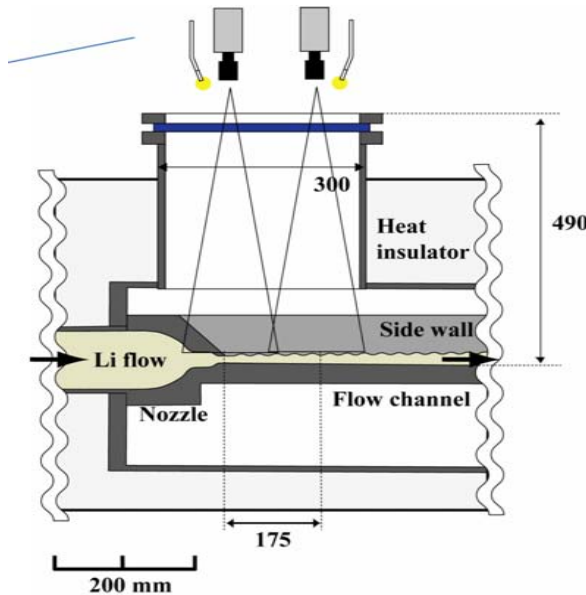
Osaka University Li test section

Li jet cross section 10mm x70mm

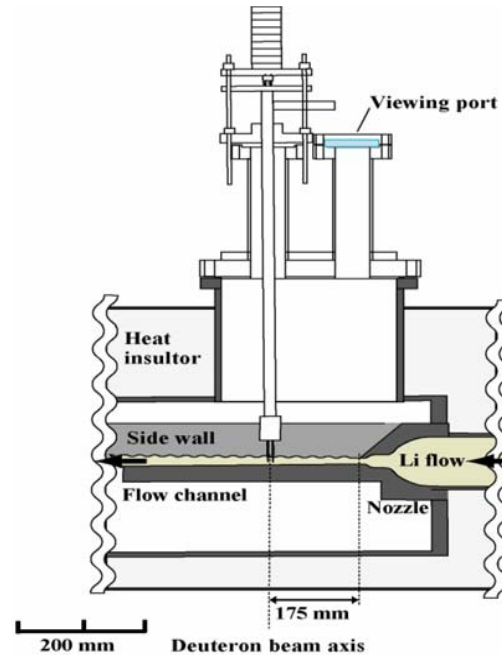
Variation of Li flow velocity at the nozzle exit: 3-15 m/s

Measurements technique and observation of the free surface flow

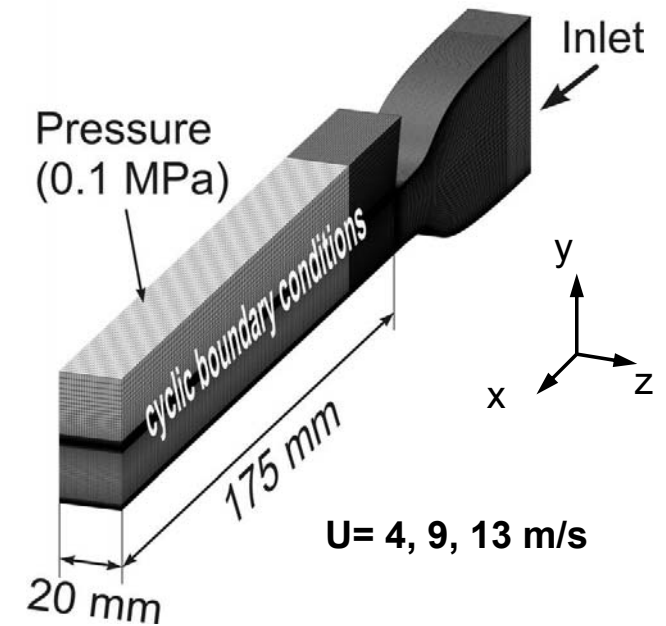
High-Speed video camera observation



Electro-contact probe method

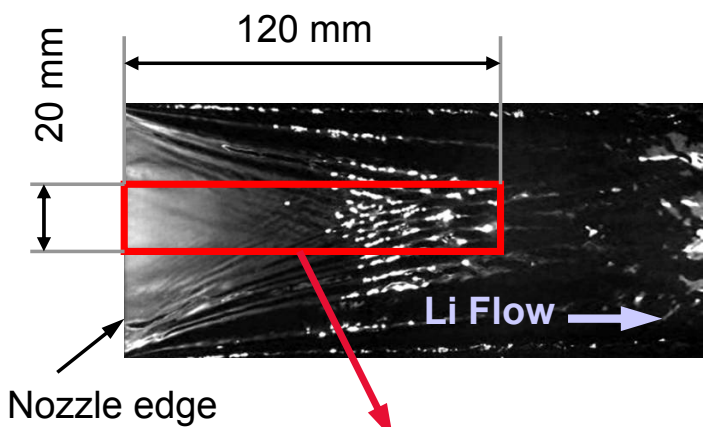


CFD model

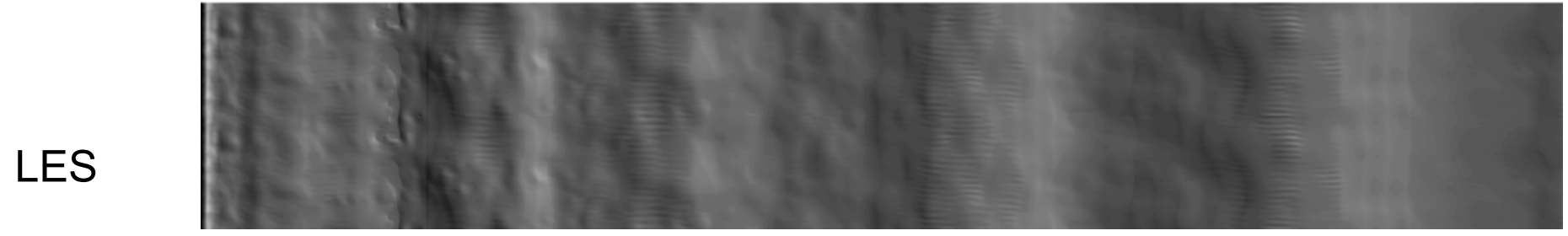
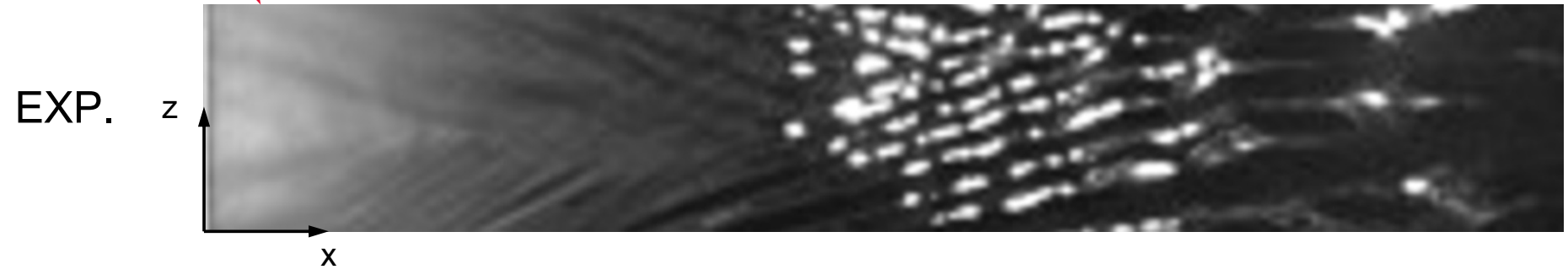
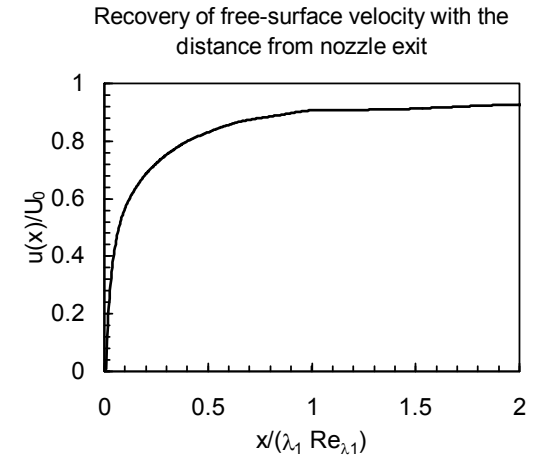


Traveling patterns. Validation of turbulence models

Comparison of HSV- photographs ($\Delta t=10\mu s$) with instantaneous VOF iso-surface

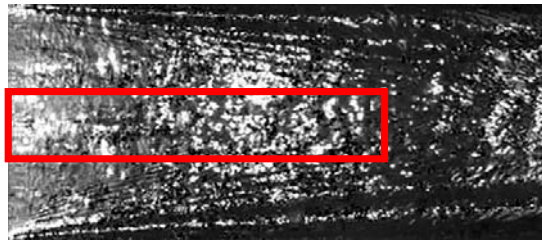


$U=4\text{m/s}$



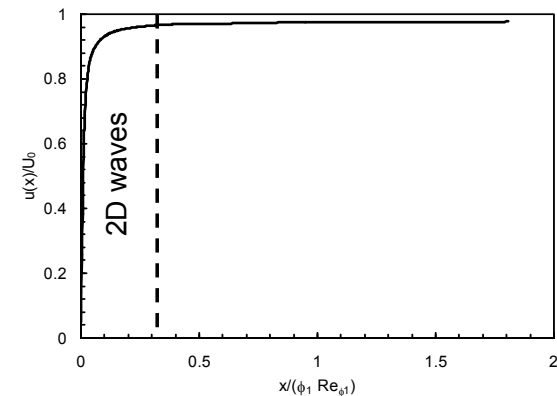
Traveling patterns. Validation of turbulence models

Comparison of HSV- photographs ($\Delta t=10\mu s$) with instantaneous VOF iso-surface



$U=9$ m/s

Recovery of free-surface velocity with the distance from nozzle exit



2D waves

3D waves

EXP.

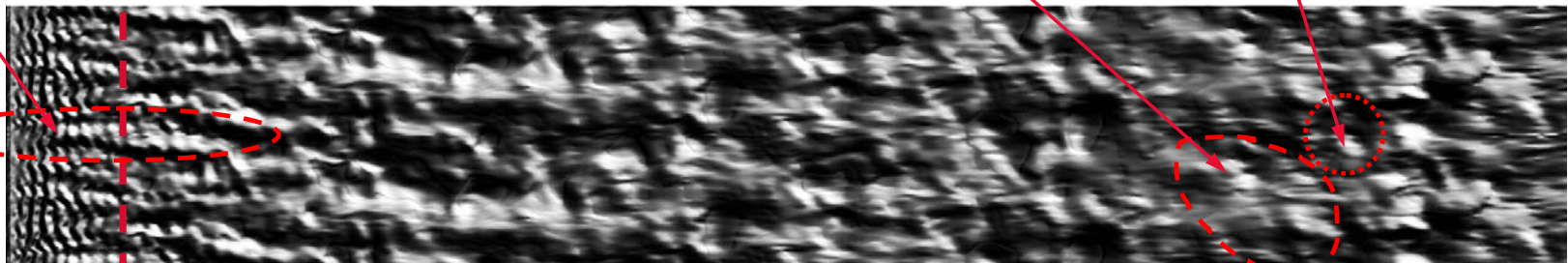


Standing waves

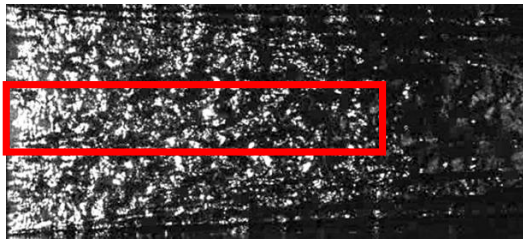
Large structures

Small structures

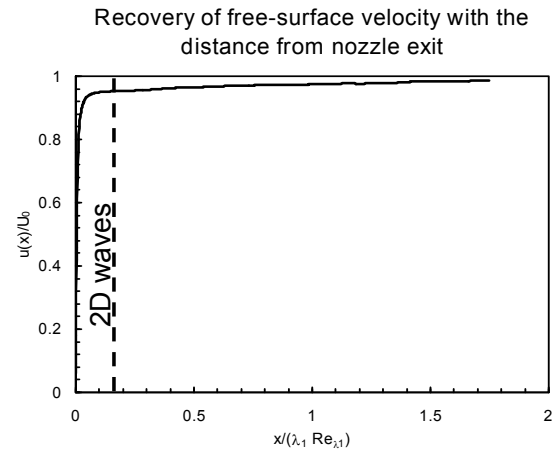
LES



Traveling patterns. Validation of turbulence models



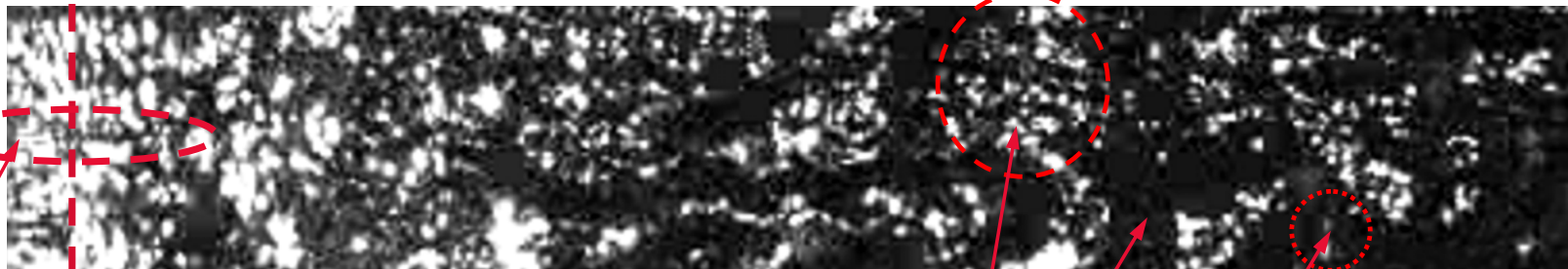
$U=13$ m/s



2D waves

3D waves

EXP.

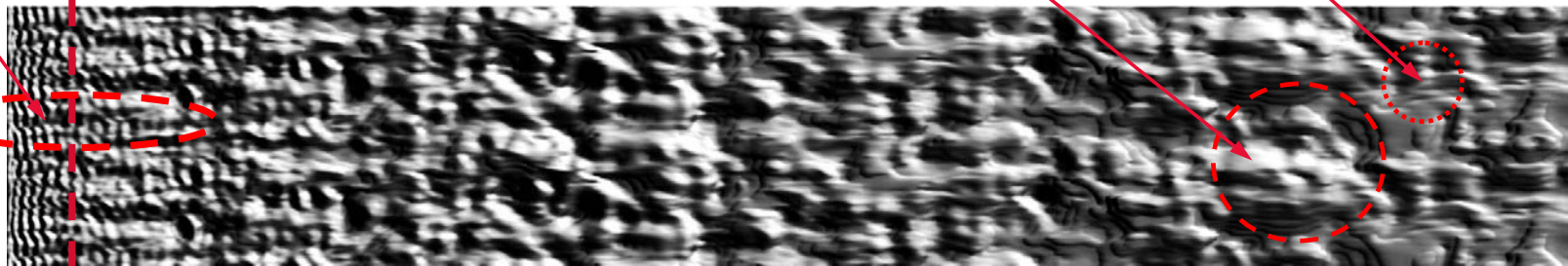


Standing waves

Large structures

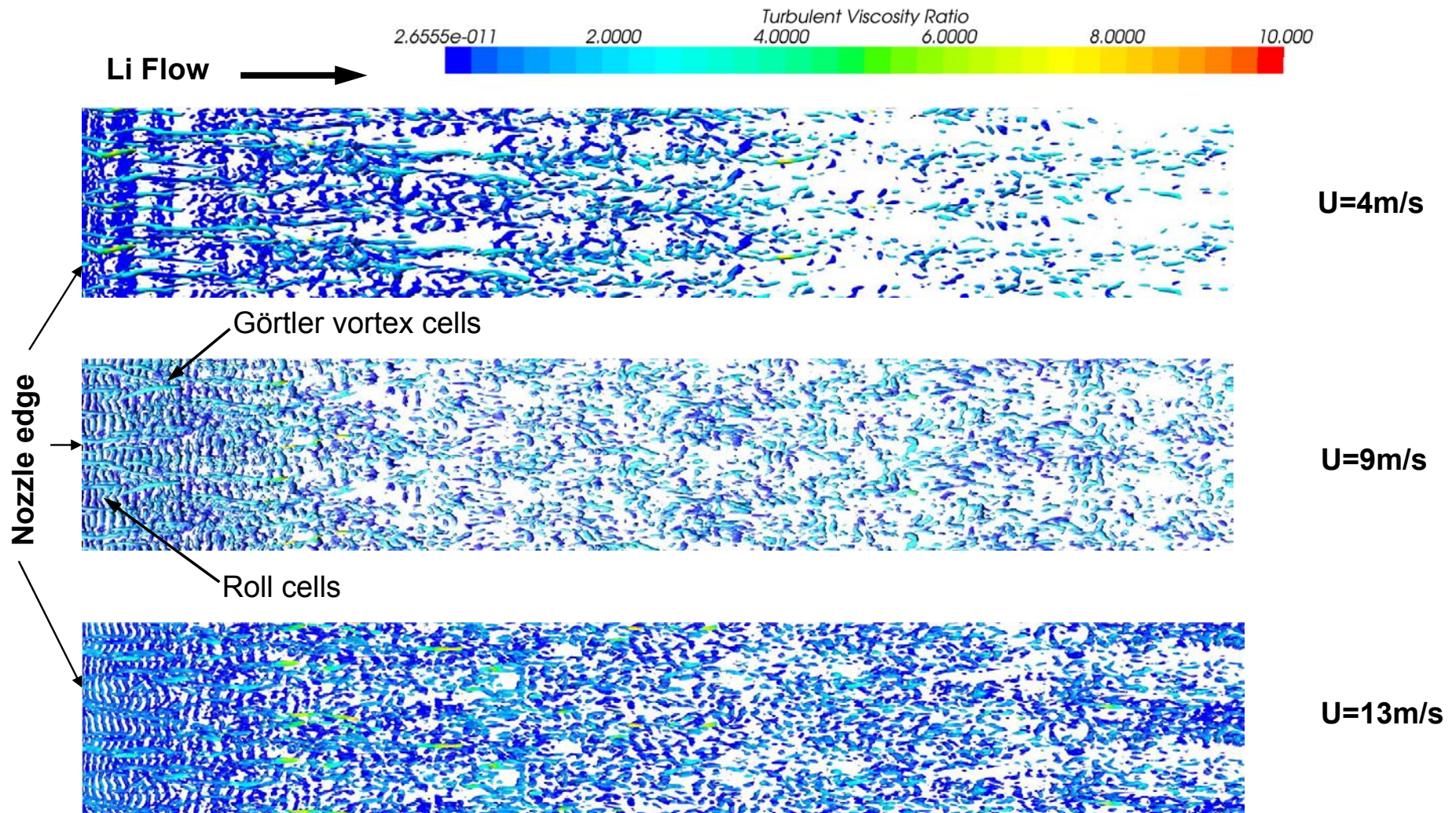
Small structures

LES



Traveling patterns. Validation of turbulence models

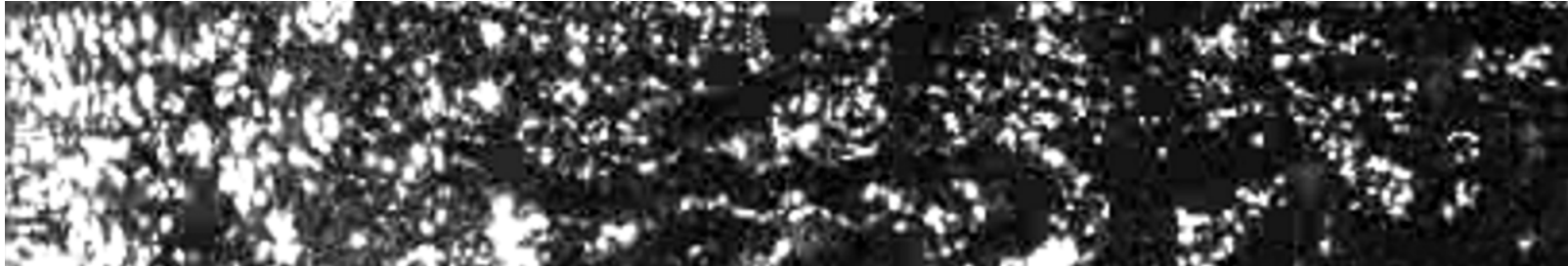
Instantaneous flow structures
iso-surfaces determined by Q-criterion close to free surface



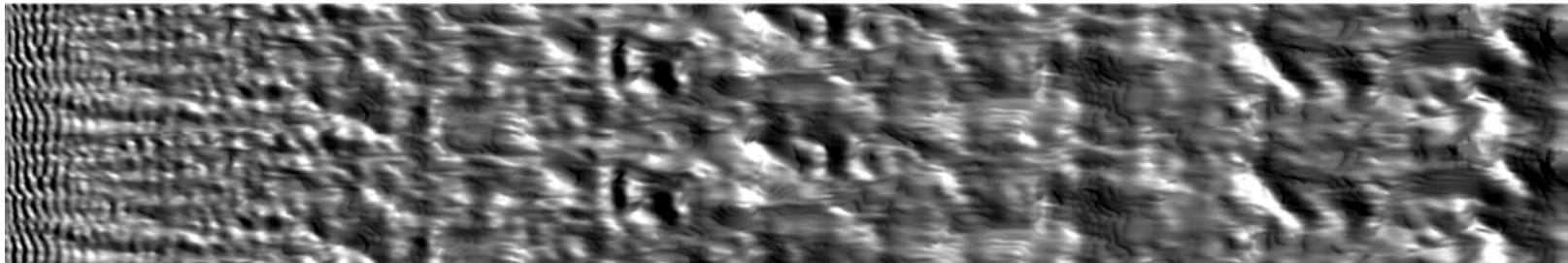
Traveling patterns. Validation of turbulence models

Comparison of HSV- photographs with instantaneous VOF iso-surfaces calculated by LES and RANS(V2F) models

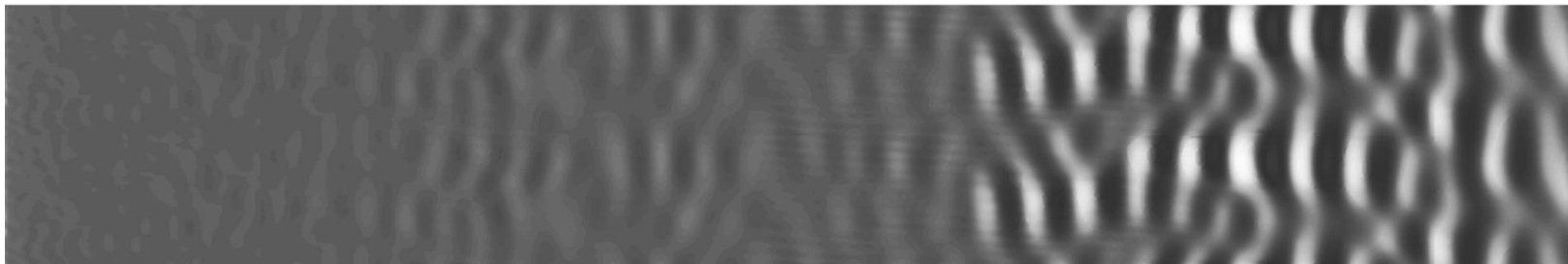
EXP.



LES

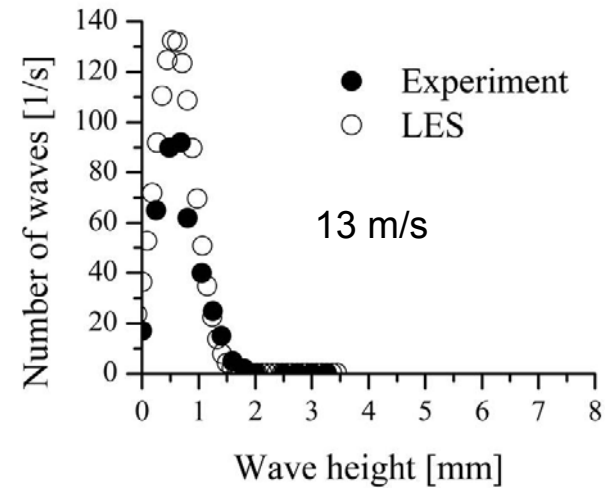
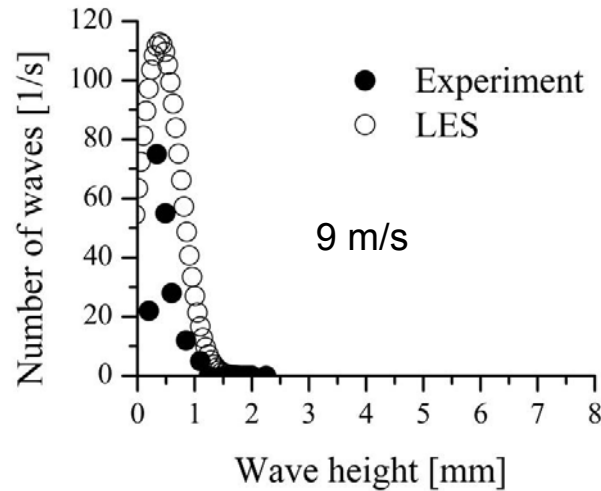


V2F

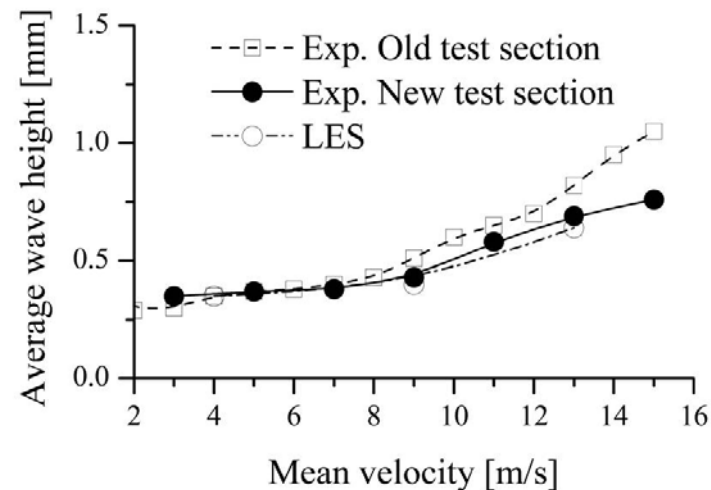


Traveling patterns. Validation of turbulence models

Wave height vs. wave number counted in one second (X=175 mm)



Average wave height of the lithium flow by old and new nozzles compared with simulations (X=175 mm)



Conclusions

- **VOF method is appropriate for simulation of liquid metal flows**
- **Appearance of waves on the free surface caused by a steady disturbances (nozzle corners, obstacles) can be predicted by both RANS and LES models with good accuracy.**
- **The interaction of waves with surface tension forces for the free-falling jet can be predicted by RANS models with good accuracy**
- **Appearance of waves caused by unsteady instability sources can be predicted only by LES models**
- **Traveling waves caused by interaction of turbulent structures with free surface can be predicted only by LES models. The accuracy of the prediction is depended on inlet conditions and grid resolution.**

Traveling patterns. Validation of turbulence models

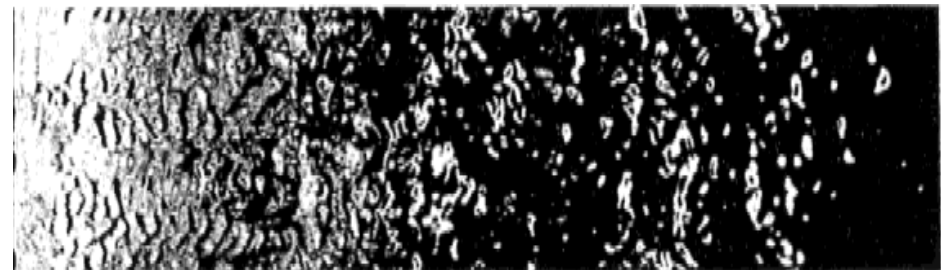
Influence of surface tension on
the surface stability

$U=4$ m/s

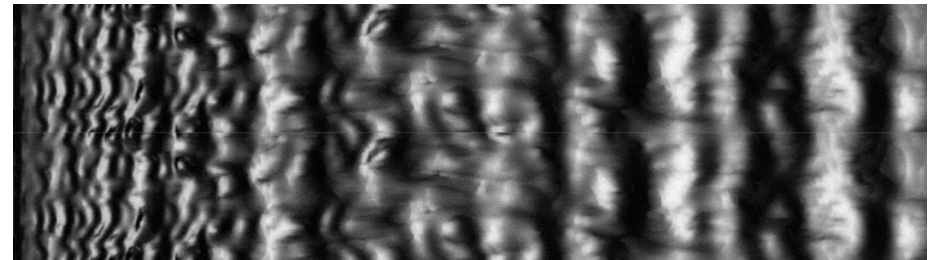
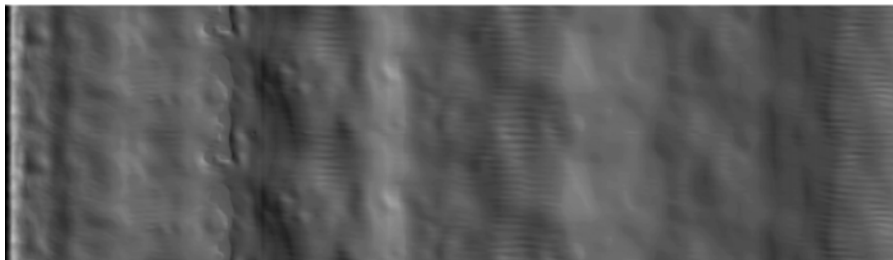
Osaka Un. Li Experiments (2010)

Nagoya Un. Water Experiments (Itoh et al., 1999)

EXP.



LES



$\sigma=0.417$ N/m, $T=300^\circ\text{C}$

$\sigma=0.073$ N/m, $T=20^\circ\text{C}$

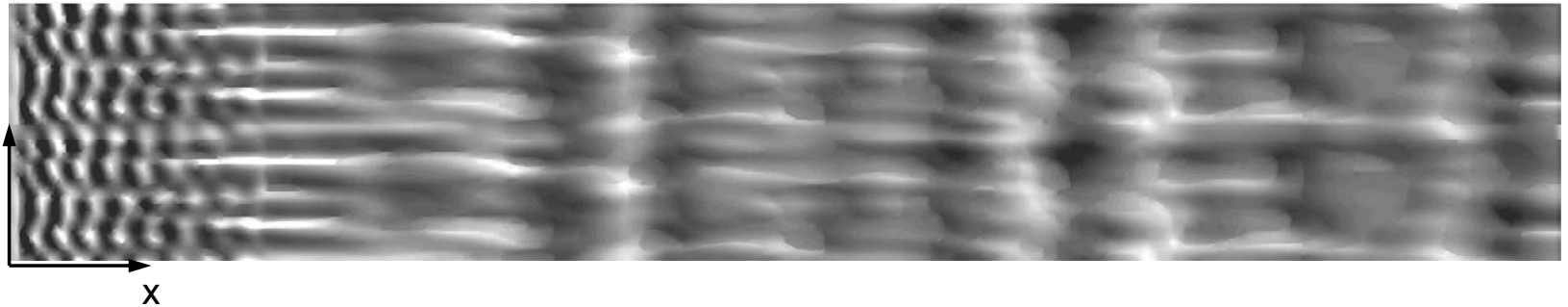
Traveling patterns. Validation of turbulence models

Grid sensitivity analysis

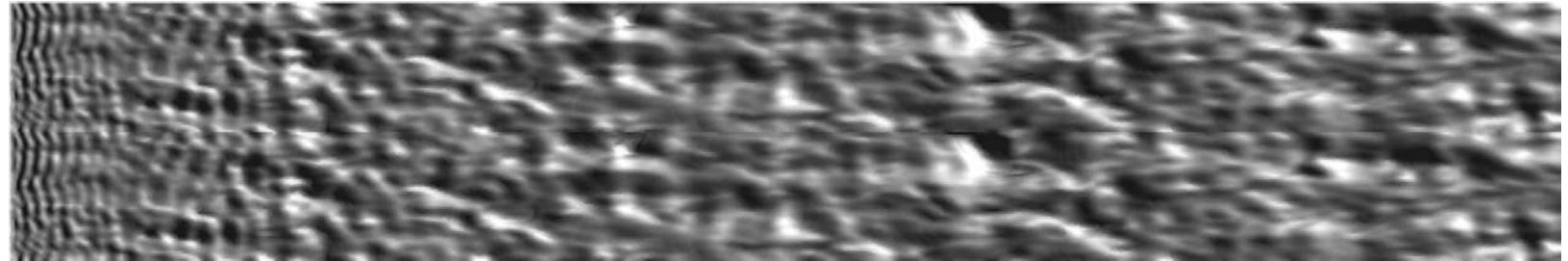
$U=13$ m/s

Grid resolution

3.65x10⁵ Cells Z
 $\Delta Z \times \Delta X = 0.5 \times 0.4$ mm



2.15x10⁶ Cells
 $\Delta Z \times \Delta X = 0.15 \times 0.2$ mm



5.65x10⁶ Cells
 $\Delta Z \times \Delta X = 0.1 \times 0.125$ mm

